Instability and Pulse Area Quantization in Accelerated Superradiant Atom-Cavity Systems

C. Greiner, T. Wang, T. Loftus, and T. W. Mossberg

Oregon Center for Optics and Department of Physics, University of Oregon, Eugene, Oregon 97403

(Received 11 June 2001; published 29 November 2001)

We study the interaction of pulsed excitation fields with optically thin atomic ensembles subject to strong cavity-accelerated superradiance. In homogeneously broadened atom-field systems the excitation of superradiant instabilities is seen to lead to a quantization of the total pulse area accrued during excitation and subsequent superradiant decay. In inhomogeneously broadened systems, quasidiscretized area values and pulse area gaps (i.e., forbidden area values) are found. Predicted area discontinuities are demonstrated in cryogenically coherence-stabilized Tm^{3+} ions.

DOI: 10.1103/PhysRevLett.87.253602 PACS numbers: 42.50.Fx, 42.50.Md, 42.65.–k

Optical excitation provides an important means of controlling the internal state of quantum systems. This is particularly true in transient settings where pulsed excitation allows for detailed quantum state preparation. A vital gauge or measure of the effect of an optical pulse on a resonant two-level system is given by the quantity known as "area" or the time-integrated product of signed optical field and atomic transition matrix element. Control over the area of an optical pulse implies control over its effect on an atomic specimen. Ordinary sources of optical pulses do not provide for direct control over area — secondary quantities such as power, temporal waveform, and temporal duration must be monitored and manipulated.

Recently, it was demonstrated [1] that a rapidly decaying cavity can be employed to dramatically accelerate the rate of Dicke superradiance [2–5] in optically thin samples. Superradiance involves a natural coupling between optical fields emitted and the internal state of atoms involved. In the present Letter, we show that atom-cavity systems supporting accelerated superradiance can exhibit the novel property of transforming input optical pulses of arbitrary area to output pulses having quantized or discrete areas. This effect is of both fundamental and practical import as area-stabilized optical sources are not readily available yet are important to areas such as quantum state preparation, quantum computing, and coherent control.

We investigate the interaction of a pulsed optical field with an optically thin ensemble of atoms subject to strong cavity-accelerated superradiance under conditions of homogeneous and inhomogeneous atomic line broadening and with traveling as well as standing-wave cavities. Optical input fields of controlled pulse area are injected along the cavity's axis creating a phased-array atomic excitation, an intracavity field, and an output field. Through cavity-accelerated superradiance, atomic emission heavily impacts intracavity and output areas. In homogeneously broadened atomic systems, superradiance leads to a quantization of the total intracavity and output pulse areas despite continuous variations in input pulse area. In inhomogeneously broadened systems, atomic emission acts to produce sharp discontinuities in intracavity and output pulse area as the injected pulse area is varied smoothly, thereby opening gaps in allowed output areas. The effects produced in both the homogeneous and inhomogeneous systems result from a superradiant instability of the atom-field system wherein the atomic ensemble relaxes rapidly to stable states and in the process controls allowed intracavity and output pulse areas. In the following, we explore the cavity-accelerated superradiant system via numerical and analytic approaches and we report experimental results providing evidence for the pulse area discontinuities predicted.

Consider a system comprising an ensemble of N initially unexcited two-level atoms located inside a unidirectional four-mirror ring cavity (Fig. 1). Two of the mirrors are partial with reflectivity R. The cavity has a photon lifetime, τ_c, which is short compared to all other system time scales, and atoms within the cavity experience a single-photon Rabi frequency, $\Omega_0/2\pi$. The relative shortness of the cavity lifetime allows us to focus on a regime of atom-cavity dynamics where the system behavior is dominated by the atomic evolution and unperturbed by cavity dynamics. The plane-wave input field has a rectangular temporal profile with a duration τ_{in} and enters the cavity at $t = 0$. Note that $\tau_{\text{in}} \gg \tau_c$. The center frequencies of the input field, atomic absorption line, and cavity resonance are coincident. The pulse areas of the input field, intracavity field, and output field are denoted θ_{in}, θ_C, and θ_{out}, respectively, where the input and output pulse areas are measured

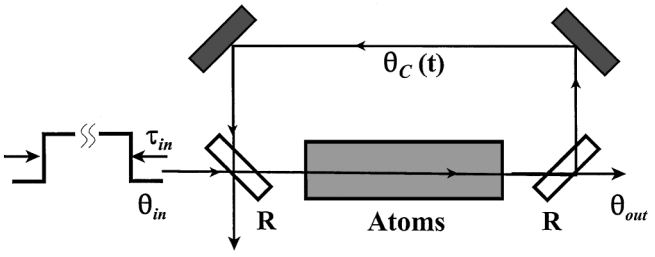

FIG. 1. Model system. R, mirror reflectivity; θ_C, θ_{in}, and θ_{out}, areas of the intracavity and cavity-external input and output fields; τ_{in}, input-pulse duration.

outside the cavity. We calculate $\theta_C(t)$, the accrued intracavity area at time t, through a numerical integration of the Maxwell-Bloch equations. System evolution is most transparent when expressed in intracavity rather than input and output quantities. For this reason, we introduce the excitation pulse area $\theta_{\rm exc} = \theta_C(\tau_{\rm in})$, which is the intracavity pulse area that accrues during the input pulse duration $\tau_{\rm in}$ and quantifies the system excitation caused by the input pulse. Note that $\theta_{\rm exc}$ is not simply proportional to $\theta_{\rm in}$ since the former includes effects of atomic emission. The total intracavity pulse area $\theta_C^{\rm tot} \equiv \theta_C(t \to \infty)$. Postexcitation superradiant emission is responsible for the difference between $\theta_C^{\rm tot}$ and $\theta_{\rm exc}$. For all calculations, homogeneous atomic decoherence and cavity loss mechanisms other than mirror transmission are ignored.

As a first model system, denoted the homogeneous system, we assume that the atoms all have the same resonance frequency. In Fig. 2, as a solid line, we plot $\theta_C^{\rm tot}$ as a function of $\theta_{\rm exc}$ for $N = 10^8$. The dashed line corresponds to the case of an empty cavity ($N = 0$). Note how continuous ranges of $\theta_{\rm exc}$ are mapped to discrete values of $\theta_C^{\rm tot} = m \times 2\pi$, where $m = 0, 1, 2, \ldots$. Transitions between different values of $\theta_C^{\rm tot}$ occur whenever $\theta_{\rm exc}$ passes through an odd multiple of π. Since $\theta_{\rm out} = \sqrt{1 - R}\,\theta_C^{\rm tot}$, quantization of $\theta_C^{\rm tot}$ implies quantization of $\theta_{\rm out}$.

The insets in Fig. 2 show the time evolution of the intracavity Rabi frequency (solid line) $\Omega_C(t) = d\theta_C(t)/dt$ and atomic inversion w (dot-dashed line) for $\theta_{\rm exc} \approx 0.73\pi$ (a) and $\theta_{\rm exc} \approx 1.1\pi$ (b). The dashed lines in the insets show the intracavity Rabi frequency generated by the input field in the absence of atoms. After the excitation ends, sustained superradiant atomic emission is observed for several microseconds. Since the cavity decay time τ_c is much shorter than the superradiant emission time τ_R, the intracavity field is driven by and follows the long-lived atomic polarization once the input field terminates. In the upper inset, where $\theta_{\rm exc} < \pi$, the superradiant emission is antiphased with respect to the excitation field, leading to zero total output pulse area. In the lower inset, where $\theta_{\rm exc} > \pi$, the sample radiates in phase with the excitation field yielding a net pulse area of 2π. The atom-field dynamics at higher thresholds are similar, except that the atoms undergo an integer number of full Rabi cycles prior to the subsequent superradiant decay. Significantly, the atomic inversion evolves back to -1 both above and below the discontinuity, indicating complete depletion of the atomic excitation energy by the superradiant process.

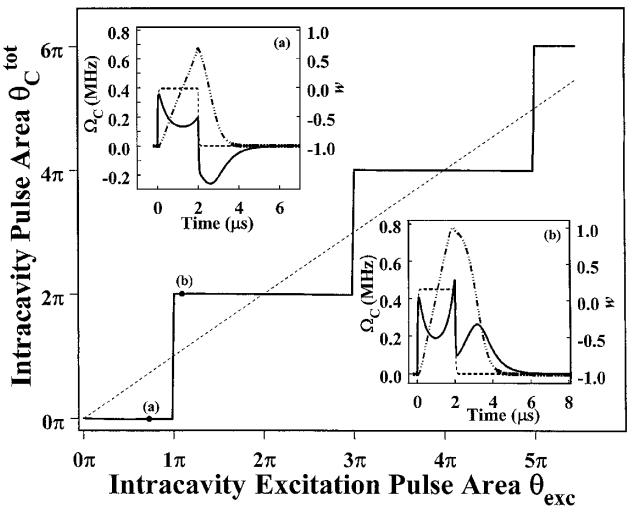

FIG. 2. $\theta_C^{\rm tot}$ versus $\theta_{\rm exc}$ for the homogeneous system. The solid and dashed lines denote the cases with and without atoms, respectively. Insets: Solid (dashed) lines, intracavity Rabi frequency Ω_C versus time with (without) atoms; dot-dashed lines, atomic inversion w versus time. Upper (lower) inset, $\theta_{\rm exc} \approx 0.73\pi$ ($\theta_{\rm exc} \approx 1.1\pi$). For all results shown, $R = 0.98$, $\Omega_0/2\pi = 100$ Hz, $\tau_c = 12$ ns, $\tau_{\rm in} = 2$ μs.

Note that the superradiance time scale, $\tau_R = 1/(\tau_c \times \Omega_0^2 \times N)$ [6], can be controlled through choice of cavity and atom parameters thereby providing a means to tailor the temporal properties of the intracavity and output fields. The area quantization effect depicted in Fig. 2 should persist even to the level of single atoms and photons as long as $\tau_R \ll T_2$, where T_2 is the homogeneous atomic decoherence time.

Inhomogeneous dephasing, present in many atomic systems, frequently obscures phenomena relying on atomic coherence. To investigate its effect on the area quantization we modify the previous system by replacing the homogeneously broadened atomic ensemble with $N \approx 3 \times 10^{10}$ atoms that are distributed across a Gaussian frequency profile with a full width at half maximum $\Delta\nu_{\rm inhom} = 90$ MHz. The inhomogeneous atomic ensemble exhibits a small signal single-pass optical thickness $\alpha L = 0.1$ at line center. Approximately 1.6×10^8 atoms are located within the excitation pulse bandwidth of $\sim 1/\tau_{\rm in}$, making the number of atoms excited here comparable to the number in the homogeneous system. A 100-ns linear rise/fall time is incorporated in the excitation pulse.

Figure 3 shows, via squares and the dashed line, respectively, $\theta_C^{\rm tot}$ as a function of $\theta_{\rm exc}$ for the inhomogeneous system with and without intracavity atoms. Strict quantization of $\theta_C^{\rm tot}$ is no longer observed. Instead, we find regions of reduced slope in the $\theta_C^{\rm tot}$ versus $\theta_{\rm exc}$ plot which are separated by abrupt discontinuous changes in $\theta_C^{\rm tot}$. The values of $\theta_{\rm exc}$ at which the discontinuities in $\theta_C^{\rm tot}$ occur are no longer uniformly spaced and differ from the homogeneous case.

Recall that in the homogeneous system $\theta_C^{\rm tot}$ discontinuities occur due to phase changes of the superradiant field when the excitation pulse drives the atom through its excited state at values of $\theta_{\rm exc} = (2m + 1) \times \pi$, where $m = 0, 1, 2, \ldots$. In contrast, in the inhomogeneous system, postexcitation superradiance is always in phase with the excitation field, yielding $\theta_C^{\rm tot} \geq \theta_{\rm exc}$ and as a consequence more subtle dynamics must underlie the discontinuities. Note that the gaps in allowed $\theta_C^{\rm tot}$ values are centered about values of $\theta_C^{\rm tot} = (2m + 1) \times \pi$. This

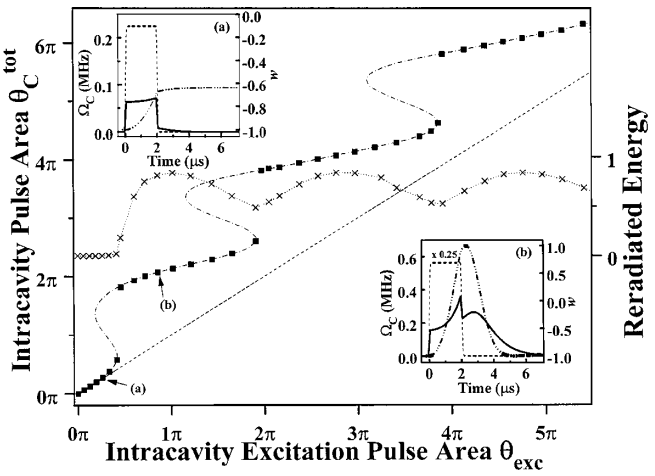

FIG. 3. θ_C^{tot} versus θ_{exc} for the inhomogeneous system. Squares and dot-dashed line (dashed line) denote the case with (without) intracavity atoms (see text). X's, fractional reradiated energy. Insets: Solid (dashed) lines, intracavity Rabi frequency Ω_C versus time for cavity with (without) atoms; dot-dashed lines, atomic inversion w at line center versus time. Upper (lower) inset, $\theta_{\text{exc}} = 0.26\pi$ ($\theta_{\text{exc}} = 0.86\pi$).

suggests that in the inhomogeneous system the discontinuities occur when the combined effect of initial excitation and postexcitation superradiance drives line-center atoms through total inversion, switching them from an absorptive to an emissive state. In contrast to the homogeneous system, postexcitation superradiance can act to increase line-center atomic excitation by virtue of superradiant release of energy stored in detuned atoms. In the insets in Fig. 3, we show the temporal dynamics of the total intracavity field and the line-center atomic inversion for values of θ_{exc} indicated. Above the θ_C^{tot} discontinuity, the line-center inversion continues to grow after the initial excitation has terminated, indicating energy transfer from detuned atoms. Subsequently, the line-center atoms superradiantly damp to the ground state while below the discontinuity they do not. Interestingly, the spectrally integrated superradiantly emitted fraction of energy absorbed from the excitation field ($\times$'s in Fig. 3) is always less than unity and exhibits oscillations correlated with the θ_C^{tot} discontinuities. The reradiated energy fraction peaks when $\theta_C^{\text{tot}} \approx 2m \times \pi$, not when area discontinuities occur.

Assuming that $\alpha L \ll 1$ and $\Delta\nu_{\text{inhom}} \gg 1/\tau_{\text{in}}$ an analytic relationship between the cavity-external input pulse area θ_{in} and the total intracavity pulse area θ_C^{tot} can be derived that provides additional insights into the dynamics of the inhomogeneously broadened system, i.e.,

$$\theta_{\text{in}} = \frac{1}{\sqrt{1-R}}\left[(1-R)\theta_C^{\text{tot}} + \frac{\alpha L}{2}\sin\theta_C^{\text{tot}}\right]. \quad (1)$$

Using numerical results to map θ_{in} onto the intracavity excitation pulse area θ_{exc}, Eq. (1) is plotted as the dot-dashed line in Fig. 3. Note how the numerical calculations are duplicated except in the regions of area discontinuity where the analytic result is multivalued. Equation (1) indicates that the θ_C^{tot} discontinuities are observable in the inhomogeneous system only if $\alpha L/2(1-R) > 1$. This condition may be compared to the premise that strong superradiant effects become appreciable only when $\alpha L \gtrsim 1$ in the absence of an accelerating cavity [7]. An analytic result analogous to Eq. (1) for a two-mirror cavity has been reported previously [8]. Here, multivalued regions were discussed in terms of the steady-state concept of optical bistability. It remains to be determined how this concept applies to the transient scenario under consideration which evolves fully deterministically suggesting single-valued mapping of specific inputs to specific outputs as observed in our simulations.

In the experiment described below, a standing-wave cavity is employed and cavity-external input and output (as opposed to intracavity) signals are measured. For comparison purposes, we present in Fig. 4, as solid squares, a relationship between the cavity-external input and output areas θ_{in} and θ_{out} calculated for a standing-wave cavity with an inhomogeneously broadened atomic ensemble. The dot-dashed line in Fig. 4 represents the multivalued analytic relationship between θ_{out} and θ_{in} calculated for this system. Single-valued portions of this relationship are highlighted by the solid line. Significantly, quasidiscretization of the output area, forbidden area regions, and discontinuities survive the strong spatial inhomogeneity of a standing-wave cavity. The insets in Fig. 4 show the Rabi frequency (solid lines) of the transmitted field and line-center inversion (dot-dashed

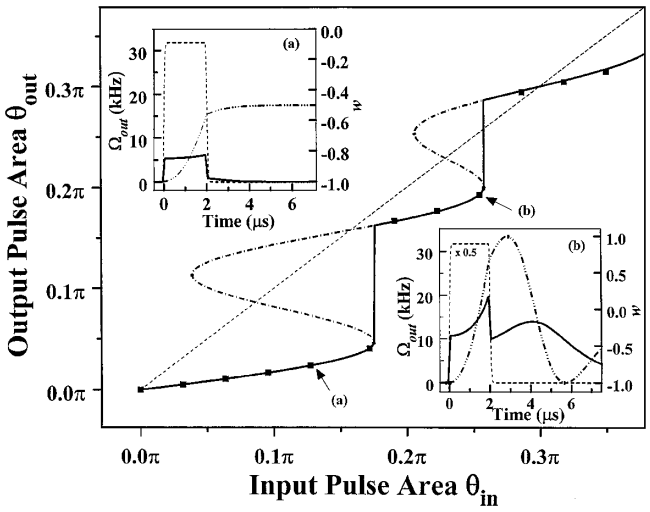

FIG. 4. θ_{out} versus θ_{in} for inhomogeneously broadened atoms in a standing-wave cavity. Squares and the dot-dashed line (dashed line) denote the case with (without) intracavity atoms (see text). Insets: Solid (dashed) lines, output Rabi frequency Ω_{out} versus time for cavity with (without) atoms; dot-dashed lines, line-center atomic inversion w at a cavity antinode versus time. Left (right) inset, $\theta_{\text{in}} = 0.13\pi$ ($\theta_{\text{in}} = 0.25\pi$).

lines) at a cavity antinode versus time both above and below the first area discontinuity. Qualitative behavior is similar to the inhomogeneously broadened but spatially homogeneous ring-cavity scenario.

To test the above predictions we have performed experiments on Tm^{3+} ions doped in a thin slice of yttrium-aluminum-garnet (YAG) crystal and located within a symmetric two-mirror standing-wave cavity [1]. The cavity parameters are $R = 0.98$, $\tau_c \approx 1.5$ ns, and $\Omega_0/2\pi \approx 170$ Hz. The ions are excited on the $^3H_6(1)$-$^3H_4(1)$ transition. The sample and cavity are cooled to ~4.6 K, where the transition has an inhomogeneous linewidth of ~20 GHz, a homogeneous dephasing time $T_2 \approx 20$ μs, an excited state ($^3H_4$) lifetime $T_1 \sim 800$ μs, and a wavelength $\lambda_{\text{air}} \approx 793.17$ nm. The single-pass line-center optical thickness, αL, is ~0.1. We estimate $N \approx 5 \times 10^8$, yielding $\tau_R \approx 1$ μs, comparable to the simulations.

The experimentally accessible quantities are the cavity-external input and output optical power as a function of time. The input field is known to be of constant phase and the theory predicts that the inhomogeneously broadened Tm^{3+} system produces an output field of constant phase. We therefore assume that $E \propto P^{1/2}$ in calculating areas from observed powers. The cavity was axially excited by a 2-μs-long pulse (rise/fall time ~100 ns) of variable amplitude (50 μW–1.6 mW). Output signals corresponding to various input powers were recorded.

The results of our measurements are shown in Fig. 5. Each solid square shown represents an average over 15 individual excitation cycles. The insets show measured output power versus time for the θ_{in} values indicated. The dashed line depicts the linear relationship between θ_{out} and θ_{in} expected in the absence of absorbers. Clear evidence of the discontinuity predicted in Fig. 4 is observed. The softness of the transition and the absence of multiple discontinuities may follow from the effects of nonuniform

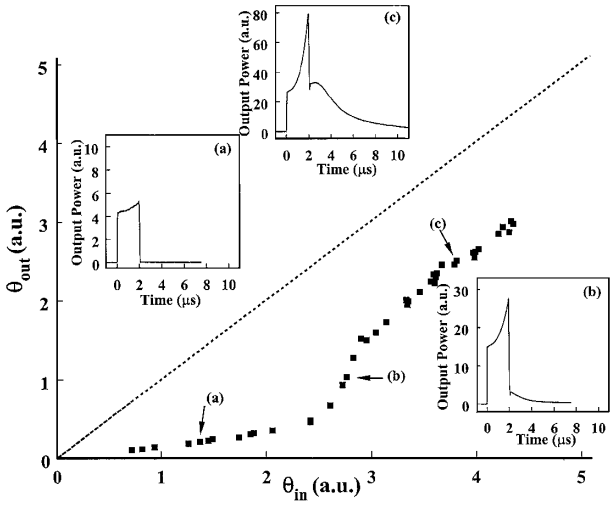

FIG. 5. Experimental data; squares (dashed line): θ_{out} versus θ_{in} with (without) atoms; insets: cavity output power versus time; the input field is on for $0 < t < 2$ μs.

transverse intensity across the cavity mode involved, homogeneous dephasing, and the presence of orientationally nonequivalent Tm^{3+} sites within the YAG host that have different atom-field coupling constants [9] and therefore experience different pulse areas.

In summary, we have explored one example of the new physics that can arise in an atomic system dominated by strong cavity-accelerated superradiance. The clamping of continuously varying input areas to discrete output areas found with homogeneous absorbers provides a powerful means of locking excitation areas to specific values regardless of fluctuations in input areas. Such a mechanism may be useful in quantum computing or other scenarios where precise and reliable atomic excitation is required. More generally, the output area discontinuities observed represent an extreme input-output nonlinearity which may provide, for example, a means of producing novel devices such as area transistors. Application of very small input area perturbations can be used to switch very large area perturbations on the output.

We appreciate support from the U.S. Air Force Office of Scientific Research under Contract No. F 49620-99-0214.

[1] C. Greiner, B. Boggs, and T. W. Mossberg, Phys. Rev. Lett. **85**, 3793 (2000).
[2] R. H. Dicke, Phys. Rev. **93**, 99 (1954).
[3] N. Skribanowitz, I. P. Herman, J. C. MacGillivray, and M. S. Feld, Phys. Rev. Lett. **30**, 309 (1973); M. Gross, C. Fabre, P. Pillet, and S. Haroche, Phys. Rev. Lett. **36**, 1035 (1976); A. Flusberg, T. Mossberg, and S. R. Hartmann, Phys. Lett. **58A**, 373 (1976); H. M. Gibbs, Q. H. F. Vrehen, and H. M. J. Hikspoors, Phys. Rev. Lett. **39**, 547 (1977).
[4] N. E. Rehler and J. E. Eberly, Phys. Rev. A **3**, 1735 (1971); R. Bonifacio, P. Schwendimann, and F. Haake, Phys. Rev. A **4**, 302 (1971); **4**, 854 (1971); R. Bonifacio and L. A. Lugiato, Phys. Rev. A **11**, 1507 (1975).
[5] Reviews on the subject can be found in M. S. Feld and J. C. MacGillivray, in *Coherent Nonlinear Optics,* edited by M. S. Feld and V. S. Letokhov (Springer, Berlin, 1980), p. 7; Q. H. F. Vrehen and H. M. Gibbs, in *Dissipative Systems in Quantum Optics,* Springer Topics in Current Physics Vol. 21, edited by R. Bonifacio (Springer, Berlin, 1982), p. 111; M. G. Benedict, A. M. Ermoloaev, V. A. Malyshev, I. V. Sokolov, and E. D. Trifonov, *Superradiance: Multiatomic Coherent Emission* (Institute of Physics Publishing, Bristol and Philadelphia, 1993).
[6] R. Bonifacio and L. A. Lugiato, Opt. Commun. **47**, 79 (1983); L. Moi, P. Goy, M. Gross, J. M. Raimond, C. Fabre, and S. Haroche, Phys. Rev. A **27**, 2043 (1983).
[7] R. Friedberg and S. R. Hartmann, Phys. Lett. **37A**, 285 (1971).
[8] S. M. Zakharov, JETP **81**, 452 (1995).
[9] C. Greiner, B. Boggs, T. Loftus, T. Wang, and T. W. Mossberg, Phys. Rev. A **60**, R2657 (1999); Y. Sun, G. M. Wang, R. L. Cone, R. W. Equall, and M. J. M. Leask, Phys. Rev. B **62**, 155 443 (2000).